molecules

MDPI

Article

Combining Temozolomide with a Selective CK2 Inhibitor Results in Anti-Tumour Effects in Glioblastoma Cell Lines

Anne S. Boewe [1,†], Hendrik Rumler [2,†], Dagmar Aichele [2], Thomas Bödeker [2], Matthias W. Laschke [1], Emmanuel Ampofo [1], Joachim Jose [2,*] and Claudia Götz [3]

[1] Institute for Clinical & Experimental Surgery, Saarland University, 66421 Homburg/Saar, Germany; matthias.laschke@uks.eu (M.W.L.)
[2] Institute of Pharmaceutical and Medicinal Chemistry, Pharma Campus, University of Münster, 48149 Münster, Germany; hendrik.rumler@posteo.de (H.R.); tboedeke@uni-muenster.de (T.B.)
[3] Medical Biochemistry and Molecular Biology, Saarland University, 66421 Homburg/Saar, Germany
* Correspondence: joachim.jose@uni-muenster.de; Tel.: +49-251-83-32200
† These authors contributed equally to this work.

Abstract

Glioblastoma is one of the most aggressive tumours with a poor prognosis and a modest survival rate after diagnosis. Several trials for a more targeted and effective treatment are in progress. Protein kinase CK2 is upregulated in glioblastoma and creates a favourable environment for cell proliferation by supporting several survival pathways. Inhibitors of CK2 kinase activity were shown to restrict growth rate or to induce apoptosis in different cell culture and animal models. Recently, we described the selective CK2 inhibitor 6,7-dichloro-1,4-dihydro-8-hydroxy-4(4 methylphenylamino)methylen]dibenzo [b,d]furan 3(2H)-one (TF). In this study, we found that TF effectively reduces the proliferation of A1207 glioblastoma cells with an EC_{50} value of 13.7 µM, which is equal to the EC_{50} value of CX-4945, which was the first CK2 inhibitor in clinical phase II trials (13.9 µM). We investigated the effect of TF and temozolomide (TMZ) as a single or combination treatment in two glioblastoma cell lines, A1207 and U87. The treatment was carried out over 48 or 72 h, and, subsequently, the biological effects were evaluated. The proliferation of both cell lines was significantly impaired by the application of the drugs, and combination treatment with TF and TMZ proved superior to the individual treatments. Not only proliferation, as determined by cell confluence assays and BrdU incorporation, but also viability in terms of metabolic activity and cytotoxicity were affected by the treatment. The decrease in proliferation and viability is partly due to the induction of apoptosis, with both cell lines differing in terms of the pattern of apoptotic caspases. Taken together, TF in combination with TMZ may be a promising candidate for the treatment of glioblastoma in the future.

Keywords: glioblastoma; temozolomide; CK2 inhibitor; CK2α knock-out; protein kinase CK2

Academic Editor: Diego Muñoz-Torrero

Received: 26 November 2025
Revised: 27 February 2026
Accepted: 5 March 2026
Published: 9 March 2026

1. Introduction

Glioblastoma (GBM) is the most common and aggressive form of adult brain cancer [1]. Due to its growth properties, GBM is classified as a grade IV tumour by the World Health Organisation (WHO) [2]. Surgery is the first-line treatment for GBM. However, complete removal of the tumour tissue is hard to achieve [3]. Hence, a combination of radiation and chemotherapy follows surgery [4]. The most common chemotherapeutic agent to treat GBM is the alkylating agent temozolomide (TMZ) [5]. The anti-tumour effect of TMZ is based on DNA methylation at the O^6 and N^7 positions of guanine, which leads

to DNA double-strand breaks. However, due to the detrimental side effects of TMZ and chemotherapy resistance [6,7], the combination of TMZ with other anti-cancer drugs is of major clinical interest. The chemotherapy resistance of tumours against TMZ is mainly due to the activity of O^6-methylguanine-methyltransferase (MGMT), which demethylates DNA at the O^6 position of methylguanine again and thus abrogates the effect of TMZ [8]. The activity of MGMT within tumour tissue is a prognostic marker for resistance development during therapy with TMZ [9].

Inhibitors of protein kinases are suitable for therapeutic applications and are often used in combination with other anti-tumour agents [10,11]. In many different tumours, protein kinase CK2 (formerly known as casein kinase 2) has been identified as a promising target for chemotherapeutic drugs [12–14]. CK2 is a constitutively active serine/threonine kinase, which is involved in several physiological and pathophysiological processes such as cell migration and cell proliferation [15,16]. CK2 is considered a key suppressor of apoptosis, a function of particular significance with respect to its role in neoplastic transformation [17]; inhibition or knock-out of CK2 should therefore increase apoptosis. The major form of CK2 is a heterotetrameric enzyme composed of two catalytically active subunits, either CK2α or its isoform CK2α′, and two regulatory β-subunits [18]. Dimerisation of two β-subunits via zinc-finger domains leads to the formation of a quaternary complex (CK2 holoenzyme) [15]. We, amongst other groups, have already reported that CK2 is upregulated in GBM cells [19,20]. Moreover, it has been shown that the gene for the catalytic subunit CK2α, CSNK2A1, was amplified in GBM tumour samples and that CK2 contributes to GBM cell survival, proliferation, migration and brain metastasis [21]. Molecular analyses revealed that this kinase regulates various pathways, including JAK/STAT, NF-κB and PI3K/Akt, and thus promotes GBM cell proliferation and migration [21]. Accordingly, the inhibition of CK2 kinase activity downregulates these processes [22,23]. In line with this view, Ferrer-Font et al. [24] demonstrated that the combination of the CK2 inhibitor CX-4945 with TMZ exerts potent anti-cancer effects in an in vivo GBM model. CX-4549 was the first CK2 inhibitor to enter clinical trials and shows an in vitro IC_{50} value towards human protein kinase CK2 of 1 nM [25]. Being an ATP-competitive inhibitor, CX-4945 also inhibits other kinases with low IC_{50} values, including, for example, CDK1, different DYRK kinases, or PIM1 [26–28]. Moreover, CX-4945 acts as a splicing modulator and may change the protein expression profile of a cell [29]. These off-target activities will complicate the assignment of CK2-specific functions but may be advantageous in chemotherapy. Although the effectiveness and benefit of CX-4945 have been reported in numerous cancer studies [25,30], this drug may lead to necrotic and apoptotic cell death [31]. Moreover, CX-4945 has also been recognised as a hazardous substance due to its potential mutagenic, carcinogenic and reproductive toxicity properties [28].

Recently, we identified the dibenzofuran scaffold as a promising lead structure for the development of novel ATP-competitive CK2 inhibitors [32–34]. A prominent member of this class of CK2 inhibitors is 6,7-dichloro-1,4-dihydro-8-hydroxy-4-[(4-methylphenylamino)-methylene]dibenzo[b,d]furan-3-(2H)-one, which is referred to as TF. TF addresses the nucleotide binding site of the catalytic α-subunit of CK2 and thus competes with the binding of the co-substrate ATP. By this mechanism, TF acts as a competitive inhibitor and reduces the enzymatic activity of CK2 without interfering with the expression of the enzyme. TF is a potent inhibitor of CK2, with a Ki value of 15 nM and an IC_{50} value of 29 nM [32]. In vitro studies demonstrated that the treatment of prostate cancer cells with TF significantly decreases cell viability and cell proliferation [32]. At the same time, treatment with TF was also tested on non-neoplastic ARPE-19 cells, revealing that viability was less impaired in normal cells than in cancer cells. Since CK2 activity is upregulated in GBM and TF exerts strong anti-cancer effects, we hypothesised that TF would enhance the anti-

proliferative effects of TMZ in GBM cells. For this purpose, we first identified an adequate concentration of TF and TMZ to reduce GBM cell proliferation. Thereafter, we studied the combined effect of TF and TMZ on cell proliferation, cell migration and apoptosis.

2. Results

2.1. Effect of TF and CX-4945 on GBM Cell Proliferation

An upregulated expression of CK2, which is often found in cancer, creates a favourable environment for the proliferation of tumour cells due to its pro-proliferative and anti-apoptotic role. Inhibiting CK2 was therefore shown to be a suitable strategy for treating cancer [35,36]. Recently, we described TF as a potent inhibitor of protein kinase CK2 (IC_{50}: 29 nM, K_I: 15 nM) [32–34]. In the present work, we analysed whether TF is an effective agent for the treatment of glioblastoma cells. In the first instance, we used A1207 glioblastoma cells [37] as a model cell line; these are malignant glioblastoma cells which were described to be temozolomide (TMZ) resistant [38,39]. The first experiment also served to compare TF with the established CK2 inhibitor CX-4945 in terms of its antiproliferative properties. Since CX-4945 is already being used as a chemotherapeutic agent in clinical phase II trials [40], we were interested in whether TF could be a serious alternative to CX-4945. For this purpose, A1207 glioblastoma cells were seeded in 96-well plates and treated with increasing concentrations of either TF or CX-4945 and DMSO as a control for 48 h. Cell confluence within the individual wells was analysed by live cell imaging. We found a significantly reduced confluence after exposure of the cells to increasing concentrations of TF or CX-4945 (Figure 1a,b). Treatment with TF showed only a minimal effect on proliferation at low doses (0.94–10 µM). However, at concentrations of 15 µM and above, no further proliferation was possible; concentrations of 20 and 30 µM even led to a decrease in the initial cell confluence. A corresponding dose–response curve for TF is shown in Figure 1c; the negative values at higher TF concentrations are due to the fact that the cell count was lower than at the start. In contrast, we observed a more proportional dose–response relationship with regard to proliferation when treating with CX-4945 (Figure 1b). Even at the highest concentration of 30 µM, the cell count did not fall below the initial number. The EC_{50} value for TF was determined to be 13.7 µM and for CX-4945 to be 13.9 µM by non-linear regression (Figure 1d). This result shows that TF is as effective in cells as CX-4945, although the in vitro efficacy of both inhibitors is different (Ki: 15 nM for TF vs. 0.38 nM for CX-4945).

To analyse the cellular uptake of TF in comparison to CX-4945, the intracellular concentration of both compounds was determined. Although not statistically significantly different, the intracellular concentration of TF appeared slightly higher compared to CX-4945 (Figure 1e). However, since no significant increase in the intracellular concentration of CX-4945 was observed between 1 and 3 µM, non-specific binding to serum proteins, the cell culture plate, and the cell membrane cannot be ruled out when determining the intracellular concentration of the inhibitor [41]. Moreover, we cannot exclude the off-target effects of TF, which may be responsible for its better performance in cellulo compared to CX-4945.

2.2. Effect of TMZ on CK2α-Deficient GBM Cell Proliferation

Based on the literature data and the observations made above, a downregulation or lack of CK2 should be useful for sensitising tumour cells towards therapeutic strategies. Therefore, we compared the expression and activity of CK2 in A1207 and A1207ΔCK2α cells; the knock-out cells, described before in [20], were generated by CRISPR-Cas9 methodology. Our results showed that CK2α is not detectable in A1207ΔCK2α cells, whereas the subunits CK2α′ and CK2β were expressed (Figure 2a). Quantification of the amount of the CK2β

subunit in A1207ΔCK2α cells demonstrated a decrease to 30% of the amount in A1207 cells (Figure 2b). The CK2 kinase activity in the knock-out cells was less than 50% when compared to A1207 cells (Figure 2c), which is due to the residual enzymatic activity of the catalytic isoform CK2α'.

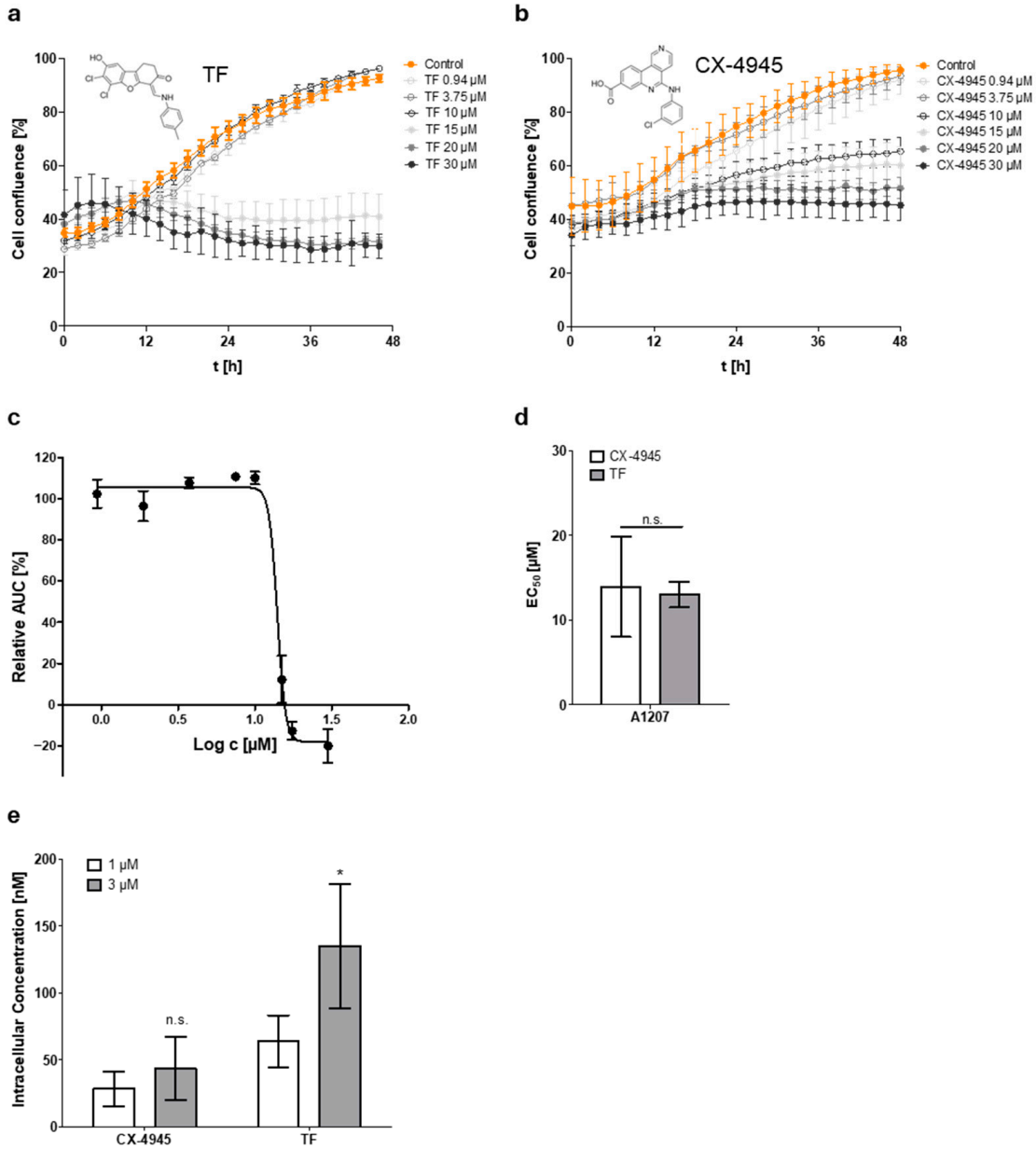

Figure 1. Anti-proliferative effects and uptake of the CK2 inhibitors TF and CX-4945 in A1207 GBM cells. (**a**). The cell confluence of A1207 cells after treatment with different concentrations of TF was monitored over 48 h using the IncuCyte® S3 live cell imaging system (mean ± SD, n = 3). (**b**). The same as (**a**) after treatment, with different concentrations of CX-4945 (mean ± SD, n = 3). (**c**). A representative dose–response curve of TF in A1207 cells. Mean values and standard deviations result from the AUCs that were determined in (**a**) and were normalised to the AUC of the control (mean ± SD, n = 3). (**d**). EC_{50} values for the respective inhibitor were determined by non-linear regression of dose–response curves (mean ± SD, n = 3, n.s.: not significant). (**e**). Cells were treated for 5 h with either 1 or 3 µM of each compound. Quantitative analysis of the intracellular concentration (nM) for each compound was performed using HPLC-MS/MS (mean ± SD, n = 3, n.s.: not significant, * $p < 0.05$).

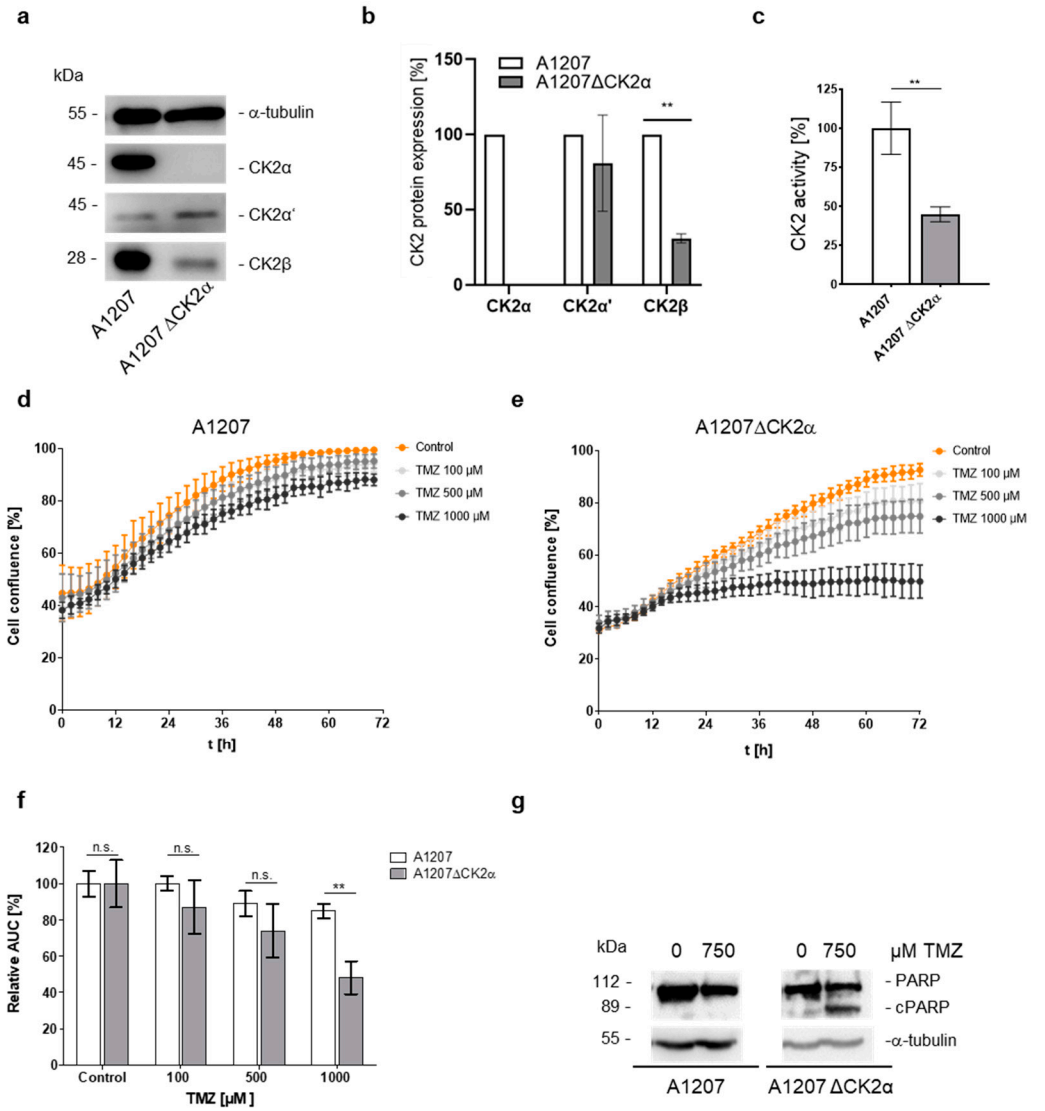

Figure 2. Effect of TMZ on CK2-deficient GBM cell proliferation. (**a**). Immunoblot analysis of A1207 and A1207ΔCK2α cell extracts was performed using CK2α, CK2α' and CK2β antibodies. α-tubulin served as a loading control. (**b**). Quantitative analysis of CK2 subunit expression from (**a**). Data are expressed in % of A1207 extracts (mean ± SD, $n = 3$, ** $p < 0.01$). (**c**). CK2 activity was determined in A1207 and A1207ΔCK2α cell extracts by a radiometric assay using the CK2-specific peptide substrate RRRDDDSDDD (mean ± SD, $n = 3$, ** $p < 0.01$). The activity of the A1207 cells was set to 100%. (**d**,**e**). Cell confluence of A1207 (**c**) and A1207ΔCK2α cells (**d**) after treatment with TMZ was monitored using the IncuCyte® S3 live cell imaging system (mean ± SD, $n = 3$). (**f**). Cell proliferation under treatment with TMZ was determined as the Area Under the Curve (AUC) relative to the control. Data are based on the confluence data from (**c**,**d**) (mean ± SD, $n = 3$, n.s.: not significant, ** $p < 0.01$). (**g**). A1207 and A1207ΔCK2α cells were treated with 750 µM TMZ or 1% (*v*/*v*) DMSO as a control, and immunoblot analysis of cell extracts was performed using a PARP antibody (cPARP: cleaved PARP). α-tubulin served as a loading control.

We next exposed the A1207ΔCK2α and A1207 cells to increasing concentrations of TMZ, and the cellular confluence was visualised by means of live cell imaging. TMZ decreased the cell proliferation of A1207 cells dose dependently (Figure 2d,f); however, it was not below 80% with the highest concentration being 1000 µM TMZ. Interestingly, this effect was more pronounced in A1207ΔCK2αcells, where proliferation almost completely ceased at the highest TMZ concentration (Figure 2e,f). To elucidate the underlying mechanism for the reduced cell proliferation, we analysed apoptosis by PARP cleavage (Figure 2g).

The results clearly indicated that it was only in the absence of CK2α that apoptosis was detectable at 750 µM TMZ. Thus, the deletion of the CK2α subunit renders A1207 cells more sensitive to TMZ treatment.

2.3. Effects of TMZ and TF Treatment on CK2 and Caspases

To further study the effect of TMZ and TF treatment on glioblastoma cells, we chose asecond human GBM model cell line, U87-MG (U87) [38]. According to [39], this cell line is TMZ responsive. Since we intended to apply the selective CK2 inhibitor to both cell lines, we first analysed the effect of the single or combined treatment with TMZ on CK2 activity and CK2 expression (Figure 3a,b). CK2 activity was reduced in both cell lines to about 60–70% with TF alone; in the presence of TMZ + TF the activity was not significantly more reduced (Figure 3a). The decrease in CK2 activity did not go along with a decrease in CK2 subunit expression (Figure 3b). Since TF is an ATP-competitive inhibitor of CK2 kinase activity, a downregulation in expression was not expected.

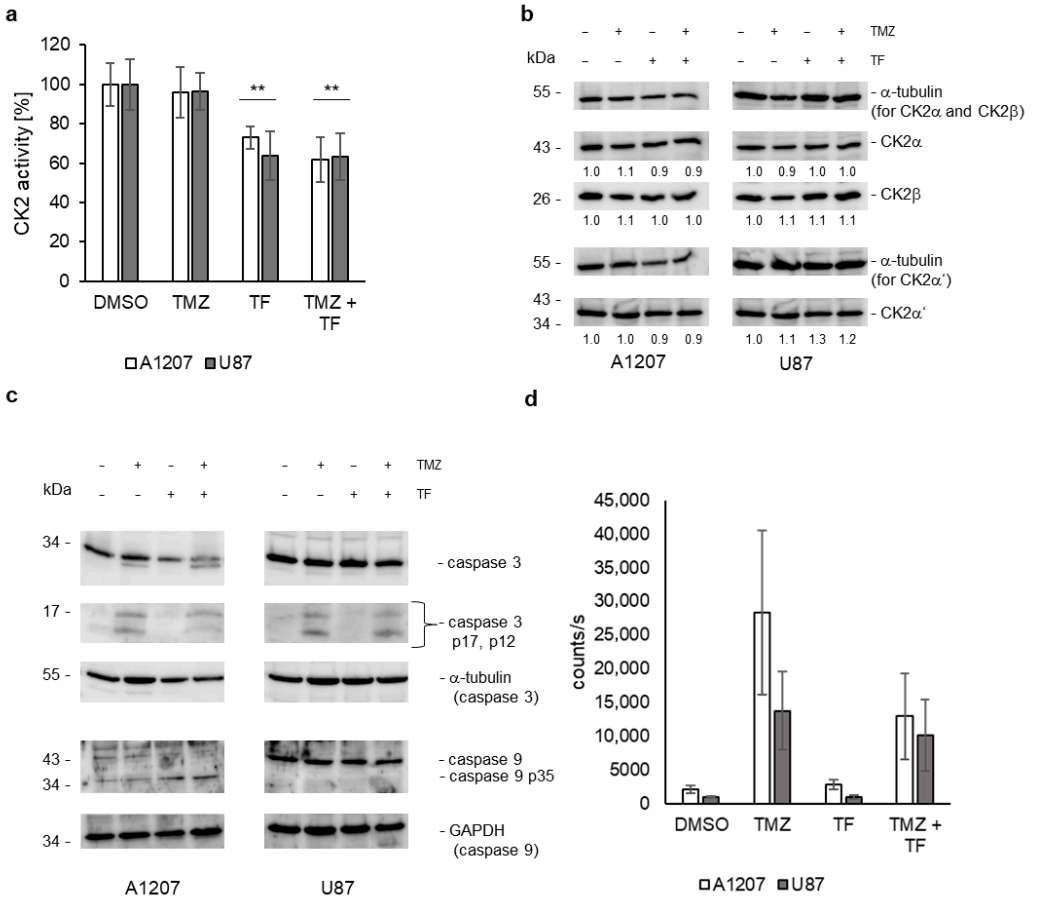

Figure 3. Effect of TMZ and TF on CK2 activity, expression and activation of caspases in GBM cell lines. A1207 and U87 cells were treated with TMZ (1000 µM) and/or TF (15 or 17.5 µM, respectively) for 48 h, harvested, extracted and analysed. (**a**). The CK2 activity was determined in A1207 and U87 cell extracts by a radiometric assay using the CK2-specific peptide RRRDDDSDDD (mean ± SD, $n = 3$, ** $p < 0.01$). The activity of the DMSO control cells was set to 100%. (**b**). The immunoblot analysis of A1207 and U87 cell extracts was performed using CK2α, CK2α′ and CK2β antibodies. α-tubulin served as a loading control. The expression ratio of the subunits after normalisation to tubulin (two independent experiments) was calculated relative to tubulin. (**c**). The immunoblot analysis of A1207 and U87 cell extracts with caspase 3 and 9 antibodies (caspase 3 p17 and p12 and caspase 9 p35 are cleavage products). α-tubulin or GAPDH served as a loading control. (**d**). The luminogenic combined caspase 3/7 activity assay of A1207 and U87 cell extracts. Luminescent signal (counts/s) is proportional to the amount of caspase activity present in cells.

As shown in Figure 2, the loss of CK2α rendered A1207 cells more sensitive to apoptosis. In the next experiment, we therefore analysed the impact of a single or combined treatment with TF and TMZ on the expression of caspases, which are key molecules of apoptosis. In more detail, we analysed caspase 3, the primary executioner caspase, together with the executioner caspase 7. Moreover, an initiator caspase of the intrinsic pathway, caspase 9, was also analysed. Activation of caspase 3 generates cleavage products with a molecular weight of 12 and 17 kDa and caspase 9 with a molecular weight of 35 kDa. Figure 3c shows that in response to TMZ alone or in combination with TF, caspase 3 is cleaved in both cell lines; single TF treatment is not able to generate an active caspase 3. The initiator caspase 9 is present in both cell lines and in an even higher amount in U87 cells. In U87 cells, it is not cleaved and thereby not activated by either TMZ or by TF treatment (Figure 3c). In A1207 cells, only a minor amount of caspase 9 is visible, which is cleaved in response to TF treatment and thereby activated (Figure 3c). Presumably, the intrinsic apoptosis signalling pathway is activated by TF in A1207 cells but not in U87 cells. In a further experiment, we analysed the combined caspase 3/7 enzymatic activity after treatment with the drugs. As shown in Figure 3d, the individual and combined treatment of both cell lines with TMZ strongly induced caspases 3 and 7, whereas the single treatment with TF did not lead to visible effects on caspases 3/7 activity.

2.4. Effect of TMZ and TF on GBM Cell Proliferation

To study the effect of TMZ and TF on cell proliferation, we performed cell confluence analyses in both GBM model cell lines, U87 and A1207. In a first step, we studied the effect of a single treatment with TMZ or TF on U87 cells; for A1207, the single treatment with both compounds was already shown (Figures 1a and 2d). We exposed U87 cells to increasing concentrations of TMZ and observed that TMZ decreased the cellular confluence dose dependently (Figure 4a); however, it did not decrease confluence below 60%, with the highest concentration being 1000 µM. With increasing concentrations of TF (Figure 4b), cell proliferation was affected beginning at a concentration of 15 µM and was significantly reduced with 17.5 µM TF. The presence of 30 µM TF did not allow any U87 cell proliferation at all. Based on this result, we calculated an EC_{50} value of 15.6 µM, which is higher than the EC_{50} value observed in A1207 cells (13 µM, Figure 1).

To define a suitable concentration of both compounds for the treatment of A1207 and U87 cells, we varied the TF concentration at a constant TMZ concentration and vice versa. In A1207 cells, single treatment with TMZ (1000 µM) led to a reduction in cell confluence to ~80% (Figure 4c). In combination with 12.5 µM TF, cell proliferation ceased after 12 h, and confluence remained constant over the 72 h measurement period (Figure 4c). In case TMZ was combined with 15 µM or 17.5 µM of TF, cell confluence started to drop after 12 h, leading to half of the initial value after 72 h in the case of 17.5 µM TF and only slightly more in the case of 15 µM (Figure 4c). The results obtained appeared similar when a constant concentration of 15 µM TF was combined with increasing concentrations of TMZ (Figure 4e). The case of 15 µM TF plus 500 µM TMZ led to a halt in cell proliferation after 12 h, with a slight recovery after 48 h. The combination of 15 µM with 750 µM or with 1000 µM of TMZ led to a decrease in cell confluence after 12 h, almost to the same extent. The results obtained with the different drug combinations in the second GBM cell line, U87, were basically the same (Figure 4d,f) with one remarkable difference: the 12 h delay of the drug effects as observed in A1207 was not visible for U87 cells. The combination of 1000 µM TMZ with 17.5 µM TF did not allow cell proliferation, and cell confluence remained constant over a period of 72 h (Figure 4d). No decrease in cell confluence, as observed for A1207 cells, was visible for any of the combinations applied over a period of 72 h (Figure 4d,f). Thus, in either case, a combination of both drugs was superior to the

treatment with the single compound, and, obviously, TF sensitised GBM cells to the TMZ treatment. In order to find out whether the combined treatment with TF + TMZ indeed had a synergistic effect, a synergy score was calculated using the public domain software SynergyFinder R (version 07.09.2024-R-3.10.3) with the Loewe model [42,43]. It turned out that, according to this model, the combination of TF + TMZ had a synergy score of 14.51 after 72 h for A1207 cells and a synergy score of 7.01 after 72 h for U87 cells. According to the software's manual, a score above 10 indicates a synergistic effect, whereas a score between −10 and +10 points indicates an additive effect. This means that TF and TMZ act synergistically in the rather TMZ resistant A1207 cell line, whereas their activities are additive in the TMZ sensitive cell line U87. Nevertheless, based on these results, in further experiments we used a combination of 1000 µM TMZ and 15 µM or 17.5 µM TF for the treatment of A1207 or U87 cells, respectively.

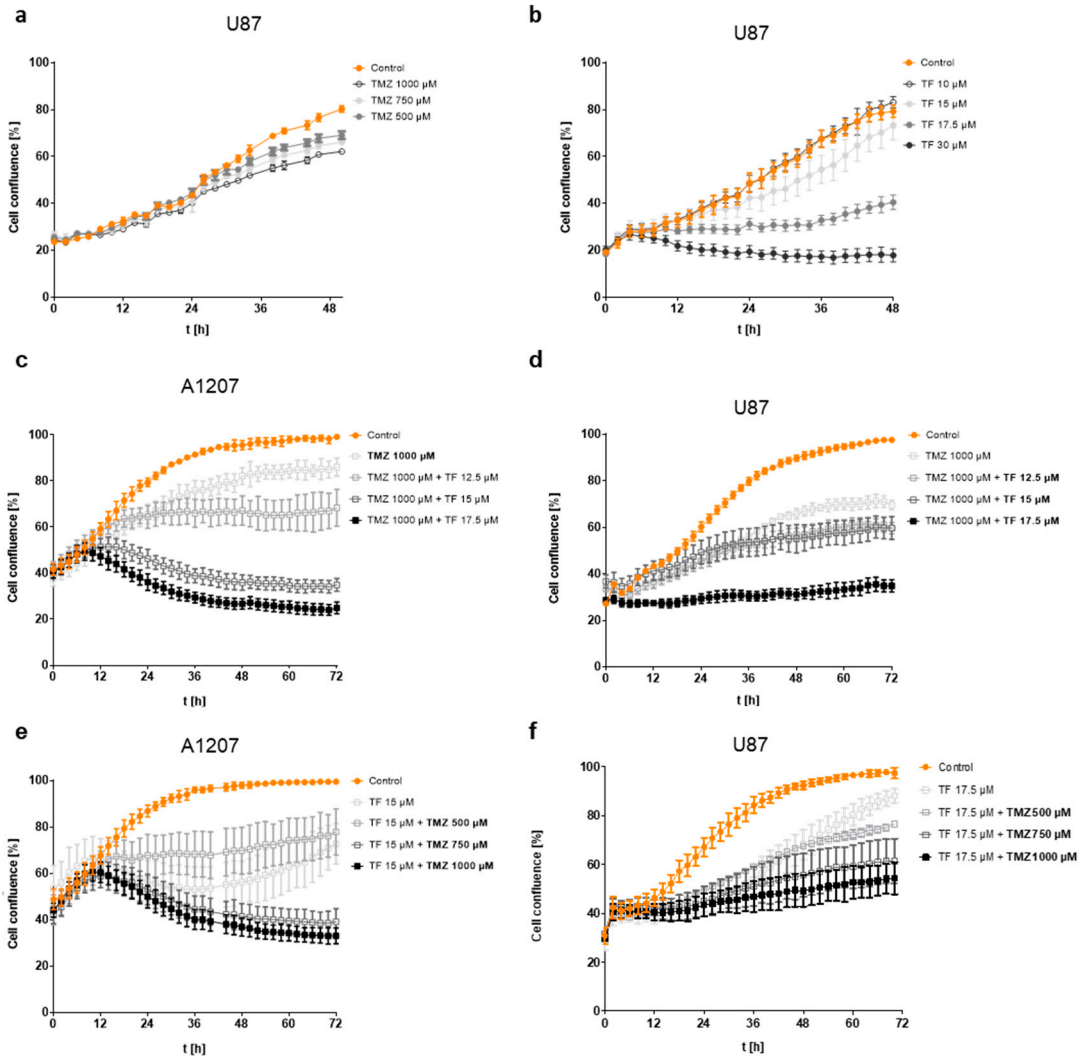

Figure 4. Effect of TMZ and TF on GBM cell proliferation. (**a**–**f**). The cell confluence was monitored after different treatments using the IncuCyte® S3 live cell imaging system over 48 h (**a**,**b**) or 72 h (**c**–**f**), respectively (mean ± SD, n = 3). Mock treatment with DMSO served as a control. (**a**). U87 cells were treated with different concentrations of TMZ. (**b**). U87 cells were treated with different concentrations of TF. (**c**,**d**). A1207 (**c**) and U87 (**d**) cells were treated with 1000 µM TMZ alone or in combination with TF in concentrations of 12.5 µM, 15 µM or 17.5 µM. (**e**). A1207 cells were treated with 15 µM TF alone or in combination with TMZ in concentrations of 500 µM, 750 µM or 1000 µM. (**f**). U87 cells were treated with 17.5 µM TF alone or in combination with TMZ in concentrations of 500 µM, 750 µM or 1000 µM TMZ.

2.5. Effect of TMZ and TF on GBM Cell Viability and Proliferation

Having shown the impact of single or combined treatment with TMZ and TF on cell confluence, CK2 expression and activity, and the pattern of different caspases in both GBM model cell lines, we further characterised the effects of the treatment on cell viability in more detail. As we had observed in cell confluence analyses of A1207 and U87 cells that the combination of TMZ and TF was always superior to the single treatment in affecting cell proliferation (Figure 4), we decided to perform further experiments with the optimal concentration of combined TMZ and TF.

Viability was analysed by WST-1 and LDH assay. For both cell lines, a minor but significantly higher level of released LDH was detectable when compared to controls (Figure 5a). The release of the enzyme LDH is a key signature of the permeabilisation of the plasma membrane and thus of the presence of necrotic cells. The cleavage of WST-1 into a coloured formazan product by metabolic activity is an indication of cell viability. As expected, treatment with TMZ and TF markedly decreased formazan production in the WST-1 assay (Figure 5b). Additional experiments analysing BrdU incorporation confirmed the anti-proliferative effect of the combined treatment of cells with both compounds (Figure 5c).

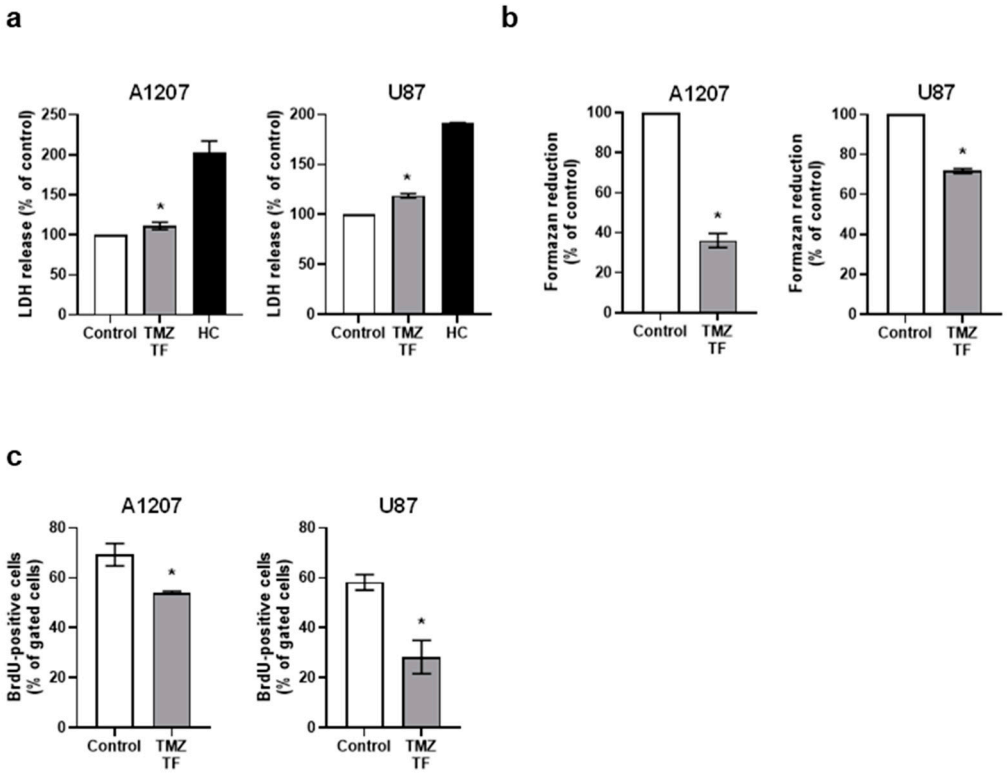

Figure 5. Effect of TMZ and TF on GBM cell viability and proliferation. (**a**–**c**). Cells were treated with a combination of 1000 µM TMZ and 15 µM (A1207) or 17.5 µM (U87) TF, respectively, or 1% (*v*/*v*) DMSO as a control for 48 h. The individual DMSO controls in the following experiments were set at 100%, and the results of the treated samples were related to this. (mean ± SD, $n = 3$, * $p < 0.05$ vs. control). (**a**). The cytotoxicity of the treatment was analysed by an LDH assay. HC: high control, giving the maximum releasable LDH activity by adding Triton X-100 solution (2% in assay medium). (**b**). The viability was measured by a WST-1 assay. (**c**). The incorporation of BrdU by proliferating cells was analysed by flow cytometry. The proportion of BrdU-positive cells was calculated based on the total number of gated cells.

2.6. Effect of TMZ and TF on Tumour Cell Migration

Finally, we analysed whether TMZ and TF also affect cell migration. For this experiment, we only chose A1207 cells for their better adherence to cell culture dishes. The effect

of 1000 µM TMZ and 15 µM TF, as single treatments or in combination, on migration was first analysed in a wound healing assay ("scratch assay"). The closure of the added gap was observed using the IncuCyte® S3 live cell imaging system over 48 h (Figure 6a,b). The individual treatments had no visible effect on the wound closure. However, the combination of both drugs significantly delayed wound healing and thus the migratory ability of the cells.

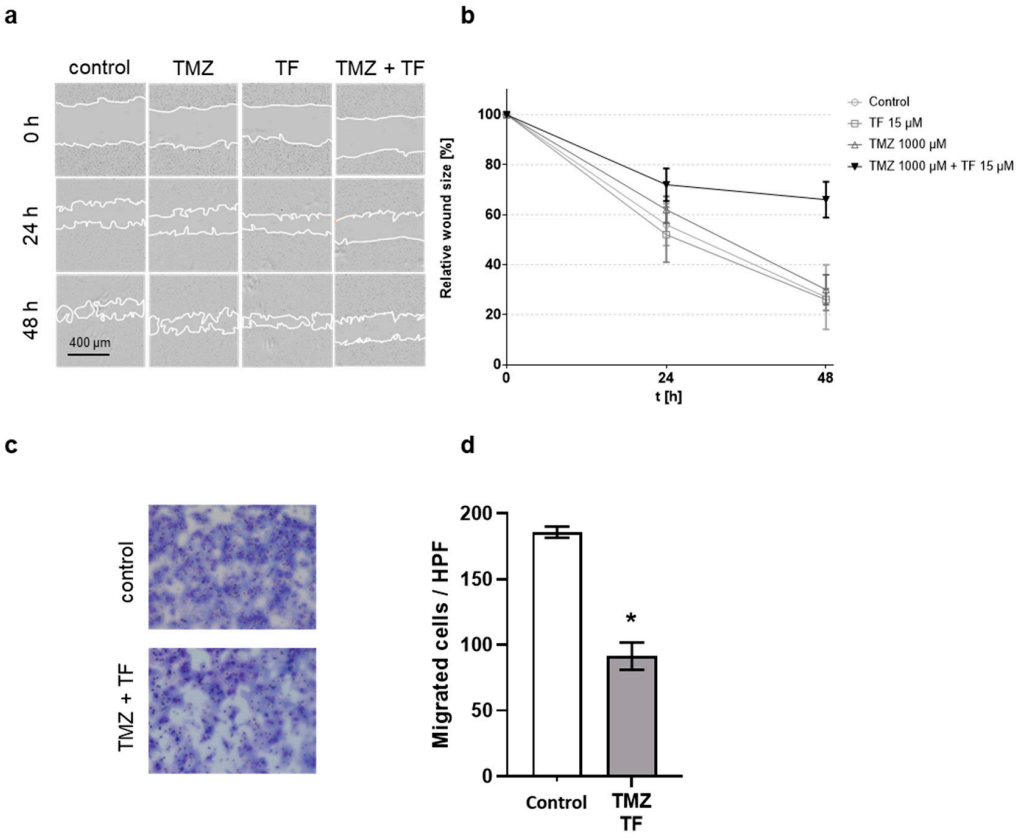

Figure 6. Anti-migratory effects of the combination of TF and TMZ in A1207 cells. (**a**). A1207 cells were cultured in 24-well plates. Scratches were added to the cell monolayer, and cells were subsequently treated with a combination of 1000 µM TMZ and 15 µM TF or with 1% (*v*/*v*) DMSO as a control for 48 h. The representative phase-contrast microscopy images showing the reduction in A1207 cell migration under treatment with TMZ and TF after 24 h and 48 h. (**b**). The quantitative analyses of the time-dependent changes in wound size of A1207 cells from (**a**) (mean ± SD, $n = 3$). (**c**). The migratory capacity was analysed using a transwell migration assay. For this purpose, 2.5×10^5 A1207 cells were seeded into the upper chamber of a 24-well chemotaxis chamber. After a 5 h incubation, migrated cells were stained and bright field images were taken (Magnification 200×). (**d**). The quantitative analyses of migrated cells from (**c**). The number of migrated cells was counted in 20 high-power fields (HPFs). The cells treated with 1% (*v*/*v*) DMSO served as a control, and the cell number was set to 100% (mean ± SD, $n = 3$, * $p < 0.05$).

A transwell assay was used to assess the ability of cells to migrate through a porous membrane (Figure 6c,d). A significantly lower number of cells (~50%) was able to migrate to the lower chamber in the presence of both compounds. Thus, this experiment supports the inhibitory effect of the combination of TMZ and TF on migration.

3. Discussion

GBM is the most common malignant brain tumour with an incidence of 2–3 new cases per 100,000 people per year. The current therapeutic strategy is the resection of the tumour, followed by a combination of radiotherapy and chemotherapy [44]. The

standard post-surgical drug is TMZ. However, ~50% of patients are resistant to TMZ therapy, which is mainly due to an increased expression of DNMT (DNA methyltransferase). The increased expression of DNMT helps maintain genomic stability, which counteracts DNA damage induced by TMZ. Accordingly, huge efforts are being made to identify alternative chemotherapeutic approaches that inhibit the destructive growth of GBM.

To study the efficacy of potential chemotherapeutic drugs in a preclinical stage, several models are available, each with individual advantages and disadvantages [38]. We chose A1207 and U87 cells for our analyses. Both cell lines are malignant glioblastoma cell lines, with A1207 [37] being rather TMZ resistant and U87 responding better to TMZ [39]. By analysing two different GBM cell lines, we hoped to arrive at a generally valid statement regarding TF as a possible treatment for glioblastoma. Moreover, we used the previously generated A1207ΔCK2α cells [20] to demonstrate the significance of CK2 for the survival of GBM cells. These cells showed a higher sensitivity towards TMZ treatment and thus underscored the meaningfulness of attacking CK2 in glioblastoma cells as a therapeutic option. However, in contrast to the CK2 inhibitor treatment, we observed a considerable downregulation of the CK2β-subunit in cells where we knocked out the catalytic α-subunit. This phenomenon is mainly due to the mutual regulation of the transcription of CK2 subunits [45,46]. Although CK2α and CK2α' are also active in the absence of CK2β, the main form of CK2 is a tetrameric holoenzyme, consisting of $CK2\alpha_2/CK2\beta_2$, $CK2\alpha\alpha'/CK2\beta_2$, or $CK2\alpha'_2/CK2\beta_2$ complexes. There are diverse functions of the regulatory subunit CK2β, such as stabilising and activating the catalytic activity of CK2, regulating substrate specificity and docking and recruiting CK2 substrates or potential regulators. Besides this role, the CK2-independent functions of CK2β have also been described, for example, CK2β being an interaction partner of the c-Mos and A-Raf protein kinases. All these findings are comprehensively summarised to a high quality in the 2003 review from D. Litchfield [15]. Based on this observation, it is likely that the results from A1207 cells treated with a CK2 inhibitor will differ from those of A1207ΔCK2α cells, as treatment with the inhibitor had no effect on the expression of the subunits during the study period.

Studies to discover adjuvant methods to treat GBM are of major clinical interest. In this context, several compounds have been identified in the last ten years that sensitise GBM cells to TMZ [47–50]. For instance, Gerlach et al. [51] found in their proof-of-concept study that the cyclotide Kalata B enhances TMZ toxicity in U87 MG and T-98G GBM cell lines. Furthermore, the Rao group [30] developed polyethylene glycol (PEG) liposomes co-loaded with TMZ and O^6-benzylguanine (O6-BG) for targeted therapy. Of interest, the dual drug-loaded liposomes exhibited superior cytotoxicity against U87 cells when compared to TMZ-treated controls [30].

Overexpression of protein kinase CK2 has been demonstrated in various cancer entities. Therefore, this enzyme has become a potential therapeutic target [14,52]. In this context, CK2 inhibition alone or in combination with other drugs has been proposed as a promising strategy for the treatment of GBM. Several in vitro and in vivo studies additionally reported that the combined treatment of GBM cells with CX-4945 and TMZ represents an effective approach to reduce cell proliferation/migration when compared with TMZ alone [24,35,47,53,54].

CX-4945 is a potent CK2 inhibitor (K_I = 0.38 nM), that is tested in phase I and II of clinical trials for the treatment of different cancer types, including cholangiocarcinoma (NCT02128282), multiple myeloma (NCT01199718) and medulloblastoma (NCT03904862). CX-4945 is a compound with a carboxyl function ((5-(3-Chloro-phenylamino)-benzo[c] [2,6] naphthyridine-8-carboxylic acid) and belongs to a rather heterogenous family of inhibitors; an IC_{50} value of 1 nM was determined for this inhibitor [55]. CX-4945 was tested with a large number of tumour cell lines, where it demonstrated a strong reduction in intracellular

CK2 activity; moreover, it is one of the most selective CK2 inhibitors known [56]. In contrast, the efficacy of CX-4945 against cancer cells is less than expected as compared to other CK2 inhibitors with IC_{50} values higher than CX-4945 [57,58]. In this context, it appears noteworthy that CK2 is implicated and modulates a number of signalling pathways dealing with the survival of a cell [59]. Studies have already reported that CX-4945 suppresses the activation of JAK/STAT, NF-kB and AKT signalling pathways in GBM [36,60,61]. We have recently shown that the expression of the proteoglycan nerve/glial antigen (NG)2 is regulated by CK2 [20,31]. It is well-known that GBM expressing NG2 is associated with a poor prognosis. This is caused by many dysregulated oncogenic pathways, such as FAK, PI3K/Akt and ERK1/2 [62]. We showed that the downregulation of CK2 activity by CX-4945 markedly reduces the expression of NG2 in GBM cell lines as well as in patient-derived GBM cell cultures due to a disturbed NG2/FAK signal [20].

We recently identified TF as a selective and potent inhibitor of CK2, with a K_I value of 15 nM, which can reduce prostate cancer cell growth [32]. TF belongs to the group of dibenzofuran derivatives that have recently been shown to represent lead structures for potent CK2 inhibitors [32–34]. Like CX-4945, TF is an ATP-competitive inhibitor. Due to the highly conserved ATP binding site of kinases, the selective inhibition of protein kinases via such inhibitors proves difficult [63]. With peptide array kinase activity profiling, it was shown that out of a panel of 61 kinases from different representative subgroups, only 7 out of 61 kinases were inhibited by more than 70% in the presence of 10 µM TF. Thus, TF shows quite a good selectivity towards CK2 [32]. The basic properties of TF treatment in normal cells and cancer cells have already been described in [32,33]. We have observed that cell viability and apoptosis induction differ in normal cells and prostate cancer cells, as normal cells are spared by TF treatment. However, at that time point, we could not exclude any cytotoxic side effects for TF, and the impact of TF on CK2-dependent signalling pathways had not yet been analysed.

The effect of TF on cell viability, proliferation and migration of other cancer types, such as GBM, has not been investigated yet. From this, we found that the treatment of A1207 cells with TF significantly reduces proliferation as significantly as CX-4945 (EC_{50} value 13.9 µM vs. 13.7 µM). The different Ki values of both inhibitors (0.38 nM vs. 15 nM) are another example that the efficacy of a small molecule inhibitor in living cells may be different from its in vitro inhibition profile [64]. Additional experiments analysing the cellular uptake of the drug showed that seemingly more TF passes the plasma membrane when compared with the same amount of CX-4945. This result, albeit, has to be handled with care. Teuscher et al. [41] convincingly demonstrated that the determination of the uptake of small molecule inhibitors is affected by a lot of uncertainties, like unspecific binding to plastic surfaces, serum proteins or metabolic stability. Preliminary subcellular distribution studies revealed that most of TF might be localised in the nucleus. Based on these results, it is tempting to speculate that the higher nuclear concentration of TF compromises the CK2-dependent modulation of the cellular transcription machinery. For instance, Sp1 regulates the expression of multiple genes, and its overexpression contributes to the malignant phenotype of GBM by upregulating genes that enhance proliferation and migration [65,66]. Sp1 is a transcription factor whose activity is influenced by the phosphorylation of CK2 [67]. Moreover, Sp1 is one of the major determinants of the promoter activity of the human protein kinase CK2α gene [68]. Interestingly, our previous studies demonstrated that the loss of CK2 decreases the activity of the transcription factor Sp1 [31]. Nevertheless, detailed analyses of the transcriptome in GBM cells after exposure to TF or CX-4945 must be performed in the future.

Notably, we only detected minor effects of the combined TMZ + TF treatment on LDH release, demonstrating that this effect is not caused by the induction of necrosis. However,

we demonstrate the induction of apoptosis by a single and a combination treatment. The key molecules in apoptosis are a group of proteases called caspases, which are themselves activated by limited proteolysis [69]. CK2 is considered an anti-apoptotic kinase; thus, the inhibition or knockout of CK2 should enhance apoptosis [17]. An overlap between the sequence of caspase substrate cleavage sites and CK2 phosphorylation motifs was demonstrated by the Litchfield group [70]. Cleavage was impeded when the motif was phosphorylated by CK2. In addition, the activating cleavage of caspase 3 is also impaired, whereby the phosphorylation of the cleavage site is attributable to the activity of CK2α′ [71].

The cleavage of PARP by caspases is an early marker for the induction of apoptosis [72,73]. We observed the cleavage of PARP in A1207ΔCK2α cells but not in A1207 cells after treatment with TMZ. This observation confirms the anti-apoptotic role of CK2. After treating A1207 and U87 with TMZ and the CK2 inhibitor TF, we therefore analysed the activation pattern of caspases. Treatment with TMZ, either alone or in combination, was associated with the activation of caspase 3, as evidenced by the cleavage of the pro-form of the enzyme. Surprisingly, we found no effect on caspase 3 activation when TF was used as a single agent. However, in A1207 cells, treatment with TF alone induced the activation of caspase 9, a key component of the intrinsic apoptosis pathway [69]. Thus, in the U87 cell line, treatment with TMZ is sufficient to induce programmed cell death; the contribution of TF to the observed stronger effect on cell proliferation cannot be explained at this time. In A1207 cells, the stronger effect on cell proliferation could be partly due to the additional induction of the intrinsic apoptosis pathway by TF, as observed by the activation of caspase 9.

Taken together, we analysed the impact of a selective CK2 inhibitor, TF, on the proliferation of two glioblastoma cell lines. The TMZ resistant A1207 cell line and the TMZ responsive U87cell line were either subjected to an individual treatment with TF or in combination with the commonly used chemotherapeutic agent TMZ. The aim of the analysis was to find out whether the simultaneous application of TF might sensitise the cells towards the TMZ treatment. Although CK2 activity was reduced to a similar extent in both cell lines, we observed differences. The EC_{50} value was determined to be 13 μM in A1207 cells and 15.6 μM in U87 cells. Consequently, the experimentally defined optimal concentration for the treatment was 15 μM TF for A1207 and 17.5 μM for U87 cells. Unexpectedly for a CK2 inhibitor, single TF treatment did not lead to caspase 3 activation in either cell line. However, in A1207 cells, the intrinsic apoptotic pathway with its key caspase 9 was induced by TF alone, which may have contributed to the stronger effect on cell proliferation. Although the underlying molecular mechanisms could not be identified more precisely, the benefit of a TMZ + TF treatment on the proliferation was clearly visible in both cell lines. The calculated synergy scores indicated an additive effect of both agents in U87 cells (synergy score 7.01) and even a synergistic effect in A1207 cells (synergy score: 14.51). Moreover, we showed that the combined treatment of GBM cells with TF and TMZ reduces cell growth without massive cytotoxic effects in cancer cells. Accordingly, TF may represent an attractive candidate for the development of novel adjuvant strategies for the treatment of GBM as well as other neoplasms.

4. Materials and Methods

4.1. Cell Culture

The human GBM cell lines A1207 (Research Resource Identifier RRID:CVCL_8481; SymbioTec GmbH, Saarbrücken, Germany [37]) and U87 (RRID: CVCL_0022; synonym: U87 MG, HTB-14™, ATCC, Manassas, VA, USA) are malignant glioblastoma cell lines. They were cultivated in a Roswell Park Memorial Institute (RPMI) medium (A1207) or a Dulbecco's Modified Eagle Medium (DMEM) (U87) that was supplemented with 10%

foetal calf serum (FCS) and penicillin–streptomycin at 37 °C and 5% CO_2 (PAN-Biotech GmbH, Aidenbach, Germany). A1207 CK2α knockout (A1207ΔCK2α) cells were generated by CRISPR-Cas9 as described previously [20] and cultivated in RPMI supplemented with 10% foetal calf serum (FCS) and penicillin–streptomycin at 37 °C and 5% CO_2. The cells were passaged at 70% confluence by a split ratio of 1:3 with trypsin-EDTA (GIBCO by Fisher Scientific GmbH, Schwerte, Germany.

4.2. Cell Proliferation Assay

To investigate the anti-proliferative effects of TF and TMZ, A1207 and A1207ΔCK2α cells were seeded at a density of 6.5×10^3 per well, and U87 cells were seeded at a density of 5×10^3 into 96-well plates. After the cells reached 40% confluence (t = 0), they were treated with TF or TMZ at the indicated concentrations (Table 1). For monitoring the cell proliferation, the IncuCyte® S3 live cell imaging system (Sartorius, Michigan, MI, USA) with a 10× objective lens was used. This is a non-invasive, image-based method to analyse cell proliferation based on the area covered with cells (cell confluence). By this method, cells of the same population within the same well are tracked continuously over time by a microscope within the incubator. In total, 25% of the whole area of a well of a 96-well plate was analysed for each condition, at least in triplicate.

Table 1. Concentrations (C) of TMZ and TF for the treatment of U87 and A1207 cells.

U87		**A1207**	
C TMZ [µM]	**C TF [µM]**	**C TMZ [µM]**	**C TF [µM]**
1000	0.0	1000	0
	12.5		12.5
	15.0		15.0
	17.5		17.5
0	17.5	0	15.0
500		500	
750		750	
1000		1000	

A software (Incucyte software tool, version 2020B) subsequently determines areas within the well that are covered by cells and calculates the proliferation based on the confluence. All controls with single compounds have been measured for 48 h, and because a stationary phase was already reached for all concentrations, these controls were not analysed any further for time points beyond. The drug combinations were measured for 72 h to see whether any additional effects could be observed. Confluence values were plotted against time points, resulting in proliferation curves of the tumour cells. The Area Under the Curve (AUC) for each concentration was calculated using Prism 8 software (GraphPad, San Diego, CA, USA).

4.3. Cellular Uptake of CK2 Inhibitors

The cellular uptake of CK2 inhibitors in A1207 cells was analysed according to the protocol published by Birus et al. [74]. The cells were treated with 1 or 3 µM of the CK2 inhibitors for 5 h. The number of cells in each sample was determined using an automated cell counter (Scepter®, Merck Millipore, Darmstadt, Germany). After centrifugation at 700× *g* and 4 °C for 5 min, cells were washed three times with phosphate-buffered saline (PBS) followed by lysis with a 100 µL lysis buffer (50 mM) Tris/HCl (pH 7.5), 1 mM

EDTA, 1 mM Na_3VO_4, 0.5 mM NaF, 0.1 mM phenylmethylsulfonyl fluoride (PMSF), 1 mM benzamidine, and 0.1% Triton (X-100). Proteins were precipitated using 500 µL ice-cold acetonitrile/methanol (ACN/MeOH) 1/1 (*v*/*v*). Samples were centrifuged for 30 min at 20,000× *g* and 4 °C. Supernatants were evaporated to dryness at 50 °C using a vacuum centrifuge maintained under full vacuum for 1.5 h. Residues were resolved in 100 µL ACN/H_2O 1/1 (*v*/*v*) and analysed via HPLC MS/MS. The intracellular concentration of the CK2 inhibitors was calculated according to Rahnel et al., 2017 [75].

$$c_x = \frac{A_x - b}{a} \times V_{final} \frac{1}{N_{cell} \times \frac{4}{3}\pi \times \left(\frac{d_{cell}}{2 \times 1.000}\right)^3} \times 1.01$$

The abbreviations in the equation are defined as follows: c_x is the intracellular concentration, A_x is the peak of the analyte, b is the intercept, a is the slope of the external calibration curve, V_{final} is the final sample volume, N_{cell} is the number of cells, and d_{cell} is the mean diameter (25 µm) of the cells.

4.4. HPLC-MS/MS Analysis

Quantitative determination of intracellular concentrations of compounds was investigated by using HPLC/MS according to the method we previously published with Birus et al. [74]. A Nexera X2 HPLC system (Shimadzu, Kyoto, Japan) was used. The system was combined with an XSelect HSS T3 analytical column (100 mm × 2.10 mm, 2.5 µm, Waters, Milford, MA, USA), maintained at 40 °C. A gradient solvent flow (A: ACN/H_2O 10/90 + 0.1% formic acid and B: ACN/H_2O 90/10 + 0.1% formic acid) was run with a flow rate of 0.3 mL/min and adjusted for analyte separation as follows:

(I) Analysis of CX-4945: 0% B to 100% B: 0.0–7.0 min; 100% B: 7.0–9.0 min; from 100% B to 0%: 9.0–9.5 min; 0% B: 9.5–15.0 min.

(II) Analysis of TF: 0% B to 100% B: 0.0–4.5 min; 100% B: 4.5–10.0 min; from 100% B to 0%: 10.0–10.5 min; 0% B: 10.5–15.0 min.

The injection volume was 5 µL. Analytes were detected with a QTrap®6500+ mass spectrometer (AB Sciex, Darmstadt, Germany), which was run in a multiple reaction monitoring (MRM) mode. The ion source was operated in an electrospray ionisation (ESI) mode. The MS parameters were optimised for the corresponding analyte in each case. Quantification was conducted using an external calibration.

4.5. Western Blotting

Western blot analysis was performed as we have described before [76]. Briefly, cells were harvested and lysed with double the volume of the RIPA buffer (50 mM Tris/HCl, pH 8.0, 150 mM NaCl, 0.5% (*w*/*v*) sodium desoxycholate, 1% (*v*/*v*) Triton X-100, and 0.1% (*w*/*v*) sodium dodecyl sulphate), which was supplemented with a complete protease inhibitor cocktail and PhosStop phosphatase inhibitor cocktail (Roche Diagnostics, Penzberg, Germany). The protein concentration was measured using a modified Bradford protein assay (Bio-Rad Laboratories, Feldkirchen, Germany). The cell extracts were separated through a 12% SDS-polyacrylamide gel and transferred onto a polyvinylidene difluoride (PVDF) membrane (Bio-Rad Laboratories). The membrane was blocked with 5% BSA in Tris-buffered saline (TBS) for 1 h. After blocking, the membrane was incubated with the indicated primary antibodies in TBS (0.1%, Tween 20 and 1% BSA, 1:1000) overnight, followed by their corresponding secondary antibodies. For loading control, we used the anti-α-tubulin antibody (cat. no. 66031) from Proteintech Germany GmbH (St. Leon-Rot, Germany) or the GAPDH-specific antibody from Santa Cruz Biotechnology (sc-25778; Heidelberg, Germany). The anti-CK2β antibody (cat. no. sc-46666) was from Santa Cruz

Biotechnology (Heidelberg, Germany). Anti-CK2α and anti-CK2α' rabbit polyclonal antisera were kindly donated by M. Montenarh [77]. As for marker proteins for apoptosis, we detected PARP and its 89 kDa cleavage product (polyclonal PARP antibody (cat. no. #9542) from Cell Signalling Technology, Frankfurt, Germany), caspase 3 and its p12 and p17 cleavage products (polyclonal rabbit antibody #9662 from Cell Signalling Technology, Frankfurt, Germany) and caspase 9 and its p35 cleavage product (rabbit polyclonal antibody, sc-8335, Santa Cruz Biotechnology (Heidelberg, Germany). The peroxidase-labelled anti-rabbit antibody (NIF 824) and peroxidase-labelled anti-mouse secondary antibody (NIF 825) were from GE Healthcare (Freiburg, Germany). The protein expression was visualised by an enhanced chemiluminescence (ECL) Western blotting substrate (Bio-Rad Laboratories) in an ECL ChemoCam Imager (Intas, Göttingen, Germany). The intensity of the measured signals was quantified using ImageJ software (version 1.54m) and normalised to the loading control (α-tubulin).

4.6. In Vitro Phosphorylation

For the determination of the kinase activity of CK2 in extracts of treated or untreated cells, the synthetic CK2-specific substrate peptide RRRDDDSDDD [78] was used [79]. The enzymatic reaction was performed using radio-labelled [^{32}P]γ ATP (Hartmann Analytic, Braunschweig, Germany) in a kinase buffer (50 mM Tris/HCl, pH 7.5, 100 mM NaCl, 10 mM $MgCl_2$, and 1 mM (DTT)) containing 20 µg protein/20 µL, which was mixed with a 30 µL reaction buffer (25 mM Tris/HCl, pH 8.5, 150 mM NaCl, 5 mM $MgCl_2$, 1 mM DTT, 50 µM ATP, and 0.19 mM substrate peptide) containing 10 µCi/500 µL [^{32}P]γ ATP (specific activity 3000 Ci/mmol and final concentration 6.7×10^{-6} mmol/L). The mixture was spotted onto a Whatman P81 ion exchange paper (Sigma-Aldrich, Munich, Germany). After washing three times with 85 mM H_3PO_4 and once with ethanol, the paper was dried, and the Čerenkov-radiation was determined in a Tricarb scintillation analyser (Packard/PerkinElmer, Waltham, MA, USA).

4.7. Caspase 3/7 Activity Assay

The cleavage activity of caspases 3 and 7 was analysed using the Caspase®-Glo Assay from Promega (Madison, Wisconsin, WI, USA). The assay contains a luminogenic caspase-specific peptide sequence, which, after cleavage, produces aminoluciferin, which in turn serves as a substrate for luciferase and thus generates luminescence.

To determine caspase activity, the cells were harvested after 48 h of treatment with TMZ and/or TF and lysed with a lysis buffer (10 mM Tris-HCl, pH 7.4, 10 mM $MgCl_2$, 150 mM NaCl, 0.5% NP-40, 1 × Complete®, and 10 mM DTT) and were incubated on ice for five minutes and then centrifuged for 10 min at 16,000× *g* and 4 °C. After determining the protein concentration, it was adjusted to 1 µg/µL with a lysis buffer and diluted to 100 ng/µL (1:10) with a protein buffer (50 mM Tris-HCl, pH 7.4, 10 mM KCl, and 5% glycerol). Next, 20 µL of the diluted protein extracts were incubated with 20 µL of Caspase-Glo® reagent for one hour at room temperature. The luminescence was recorded using a Tecan Spark 20M multimode microplate reader (Tecan Trading AG, Männedorf, Switzerland).

4.8. Lactate Dehydrogenase (LDH) Assay

A lactate dehydrogenase (LDH) assay was used to evaluate the cytotoxic effect of TMZ and TF on A1207 and U87 cells, as described before [20]. For this, the cells were seeded in a 96-well culture plate at a density of 2×10^3 cells/well and treated with TMZ and TF or DMSO. After 48 h, the assay was performed according to the manufacturer's instructions (Cytotoxicity detection kit, Roche, Mannheim, Germany) and the absorbance was measured at 482 nm in a Tecan Infinite 200 Pro microplate reader (Tecan, Crailsheim, Germany).

4.9. Water-Soluble Tetrazolium (WST)-1 Assay

A WST-1 assay (Roche) was used to analyse the effect of TMZ and TF on the metabolic activity and thus on the viability of A1207 and U87 cells. In this assay, formazan is the product formed by mitochondrial dehydrogenases in metabolically active cells from a tetrazolium salt that is added as a substrate. Briefly, the cells were seeded in a 96-well culture plate at a density of 2×10^3 cells/well and treated with TMZ and TF or DMSO. After 48 h, 10 µL of WST-1 reagent was added to each well and the absorbance was measured at 450 nm in a Tecan Infinite 200 Pro microplate reader (Tecan, Männedorf, Switzerland).

4.10. Bromodeoxyuridine (BrdU) Assay

A BrdU assay was used to assess the effect of TMZ and TF on cell proliferation. Briefly, A1207 and U87 cells were treated with TMZ and TF or DMSO for 48 h and exposed to 10 µM BrdU (Roche) for 10 h. Thereafter, the cells were fixed, permeabilised, and incubated with an anti-5-bromo-2′-deoxyuridine (BrdU) antibody (eBioscience by Thermo Fisher Scientific, Karlsruhe, Germany). The percentage of BrdU-positive cells was analysed by a FACSLyric™ flow cytometer (BD, Heidelberg, Germany).

4.11. Transwell Migration Assay

A transwell migration assay was used, as we have described before [20], to analyse the effect of TMZ and TF on the migratory capacity of A1207 cells. For this purpose, 24-well chemotaxis chambers with polycarbonate filters (pore size of 8 µm) (Corning, New York, NY, USA) were preincubated (overnight) in a culture medium without any supplements. Thereafter, the medium was removed, and 750 µL of the culture medium was supplemented with 5% FCS and added to the bottom well. Subsequently, the cells (2.5×10^5 cells in 200 µL culture medium (0.1% FCS)) were seeded into the upper chamber and incubated for 5 h. Non-migrated cells were removed by cotton swabs, and migrated cells were stained with Dade Diff-Quick (Dade Diagnostika, Munich, Germany). The number of migrated cells was counted in 20 high-power fields (HPF) (BZ-8000; Keyence, Osaka, Japan). The HPF were schematically selected as 5 adjacent fields per row in 4 consecutive rows. High Power Field (HPF) refers to the area visible through a microscope at high magnification, here 200× magnification.

4.12. Tumour Cell Migration Analysis (Wound Healing or "Scratch Assay")

A1207 cells were cultured in 24-well plates, which were pre-coated with 300 µg/mL of collagen-I in 0.02 M acetic acid for better adherence. Cells were seeded at densities of 5×10^4 per well (24-well plate) and cultured at 37 °C and 5% CO_2 until 100% confluence. Scratch wounds were created using a 200 µL pipette tip. Cells were washed twice using 500 µL pre-warmed medium. Subsequently, cells were treated with either 1000 µM TMZ or 15 µM TF, which was the combination of 1000 µM TMZ and 15 µM TF or vehicle control (1% DMSO). Phase contrast images at 0 h, 24 h and 48 h were taken using the IncuCyte® S3 live cell imaging system (Sartorius) with a 4× objective lens. The wound size in each well was determined using the Wound Healing Size Tool of the ImageJ 1.50i software. The wound size at each time point was normalised to the wound size at 0 h to obtain the relative wound size.

4.13. Statistical Analysis

After testing the data for normal distribution and equal variance, the differences between the two groups were assessed by the unpaired Student's *t*-test. Statistics were performed by GraphPad Prism (Prism 8 software, GraphPad, San Diego, CA, USA). All the values are expressed as the mean ± SD. Statistical significance was accepted for $p < 0.05$.

5. Conclusions

In the present study, it is shown that the combination of the DNA-alkylating agent TMZ, already in use for GBM treatment, with the potent human protein kinase CK2 inhibitor TF, leads to an improved reduction in tumour cell proliferation, viability, and migration in glioblastoma cell lines. By applying these experiments to a CK2α knock-out cell line, it was shown that this effect is indeed due to CK2 inhibition. The cell culture data as obtained appear to be promising, but for a potential therapeutic treatment using a combination of TMZ and TF, further important obstacles need to be overcome. Although it is known that TMZ is orally available and able to cross the blood–brain barrier (BBB), the oral availability and the BBB permeability of TF still need to be investigated. In cases where only minor amounts of TF can pass the BBB, its restricted solubility could be an obstacle for oral administration. In such cases, alternative formulations for drug delivery need to be taken into consideration. Other pharmacokinetic properties, such as metabolic stability, need to be evaluated as well, before a combined treatment of GBM with TMZ and TF can be considered. In conclusion, several further experiments are required to evaluate the in vivo perspectives of a combined TMZ/TF treatment for GBM, but the cellular data as presented here make it appear worthwhile.

Author Contributions: Conceptualisation, E.A., C.G. and J.J.; methodology, A.S.B., H.R., T.B. and C.G.; validation, D.A., C.G. and E.A.; formal analysis, D.A., C.G. and E.A.; investigation, A.S.B., H.R., T.B. and C.G.; resources, M.W.L., E.A., C.G. and J.J.; writing—original draft preparation, A.S.B., H.R., D.A., C.G. and E.A.; writing—review and editing, D.A., C.G., E.A., and J.J.; visualisation, A.S.B., H.R., D.A., T.B. and C.G.; supervision, E.A., D.A., and J.J.; project administration, J.J. All authors have read and agreed to the published version of the manuscript.

Funding: This research received no external funding.

Institutional Review Board Statement: Not applicable.

Informed Consent Statement: Not applicable.

Data Availability Statement: Dataset available on request from the authors.

Acknowledgments: We would like to thank Mathias Montenarh for kindly donating polyclonal rabbit antisera against CK2 and for critically reading the manuscript.

Conflicts of Interest: The authors declare no conflicts of interest.

Abbreviations

The following abbreviations are used in this manuscript:

ACN	Acetonitrile
AUC	Area Under the Curve
BBB	Blood–Brain Barrier
BrdU	Bromodeoxyuridine
CK2	Protein Kinase CK2, formerly known as casein kinase 2
DNMT	DNA Methyltransferase
GBM	Glioblastoma
LDH	Lactate Dehydrogenase
MGMT	O^6-methylguanine-methyltransferase
NG2	Nerve/glial antigen 2
PARP	Poly(ADP-ribose)-polymerase
TF	6,7-dichloro-1,4-dihydro-8-hydroxy-4(4 methylphenylamino)methylen]dibenzo [b,d]furan 3(2H)-one
TMZ	Temozolomide
WST-1	Water-Soluble Tetrazolium (WST)-1

References

1. Tan, A.C.; Ashley, D.M.; López, G.Y.; Malinzak, M.; Friedman, H.S.; Khasraw, M. Management of glioblastoma: State of the art and future directions. *CA Cancer J. Clin.* **2020**, *70*, 299–312. [CrossRef]
2. Louis, D.N.; Perry, A.; Reifenberger, G.; von Deimling, A.; Figarella-Branger, D.; Cavenee, W.K.; Ohgaki, H.; Wiestler, O.D.; Kleihues, P.; Ellison, D.W. The 2016 World Health Organization Classification of Tumors of the Central Nervous System: A summary. *Acta Neuropathol.* **2016**, *131*, 803–820. [CrossRef]
3. McKinnon, C.; Nandhabalan, M.; Murray, S.A.; Plaha, P. Glioblastoma: Clinical presentation, diagnosis, and management. *BMJ* **2021**, *374*, n1560. [CrossRef]
4. Keime-Guibert, F.; Chinot, O.; Taillandier, L.; Cartalat-Carel, S.; Frenay, M.; Kantor, G.; Guillamo, J.S.; Jadaud, E.; Colin, P.; Bondiau, P.Y.; et al. Radiotherapy for glioblastoma in the elderly. *N. Engl. J. Med.* **2007**, *356*, 1527–1535. [CrossRef] [PubMed]
5. Fresnais, M.; Turcan, S.; Theile, D.; Ungermann, J.; Abou Zeed, Y.; Lindner, J.R.; Breitkopf, M.; Burhenne, J.; Haefeli, W.E.; Longuespée, R. Approaching Sites of Action of Temozolomide for Pharmacological and Clinical Studies in Glioblastoma. *Biomedicines* **2021**, *10*, 1. [CrossRef] [PubMed]
6. Friedman, H.S.; Kerby, T.; Calvert, H. Temozolomide and treatment of malignant glioma. *Clin. Cancer Res.* **2000**, *6*, 2585–2597.
7. Hombach-Klonisch, S.; Mehrpour, M.; Shojaei, S.; Harlos, C.; Pitz, M.; Hamai, A.; Siemianowicz, K.; Likus, W.; Wiechec, E.; Toyota, B.D.; et al. Glioblastoma and chemoresistance to alkylating agents: Involvement of apoptosis, autophagy, and unfolded protein response. *Pharmacol. Ther.* **2018**, *184*, 13–41. [CrossRef]
8. Esteller, M.; Garcia-Foncillas, J.; Andion, E.; Goodman, S.N.; Hidalgo, O.F.; Vanaclocha, V.; Baylin, S.B.; Herman, J.G. Inactivation of the DNA-repair gene MGMT and the clinical response of gliomas to alkylating agents. *N. Engl. J. Med.* **2000**, *343*, 1350–1354. [CrossRef]
9. Weller, M.; van den Bent, M.; Preusser, M.; Le Rhun, E.; Tonn, J.C.; Minniti, G.; Bendszus, M.; Balana, C.; Chinot, O.; Dirven, L.; et al. EANO guidelines on the diagnosis and treatment of diffuse gliomas of adulthood. *Nat. Rev. Clin. Oncol.* **2021**, *18*, 170–186. [CrossRef] [PubMed]
10. Grygier, P.; Pustelny, K.; Nowak, J.; Golik, P.; Popowicz, G.M.; Plettenburg, O.; Dubin, G.; Menezes, F.; Czarna, A. Silmitasertib (CX-4945), a Clinically Used CK2-Kinase Inhibitor with Additional Effects on GSK3β and DYRK1A Kinases: A Structural Perspective. *J. Med. Chem.* **2023**, *66*, 4009–4024. [CrossRef]
11. Trembley, J.H.; Kren, B.T.; Afzal, M.; Scaria, G.A.; Klein, M.A.; Ahmed, K. Protein kinase CK2—Diverse roles in cancer cell biology and therapeutic promise. *Mol. Cell. Biochem.* **2023**, *478*, 899–926. [CrossRef]
12. Ortega, C.E.; Seidner, Y.; Dominguez, I. Mining CK2 in cancer. *PLoS ONE* **2014**, *9*, e115609. [CrossRef] [PubMed]
13. Chen, Y.; Wang, Y.; Wang, J.; Zhou, Z.; Cao, S.; Zhang, J. Strategies of Targeting CK2 in Drug Discovery: Challenges, Opportunities, and Emerging Prospects. *J. Med. Chem.* **2023**, *66*, 2257–2281. [CrossRef]
14. Chua, M.M.; Ortega, C.E.; Sheikh, A.; Lee, M.; Abdul-Rassoul, H.; Hartshorn, K.L.; Dominguez, I. CK2 in Cancer: Cellular and Biochemical Mechanisms and Potential Therapeutic Target. *Pharmaceuticals* **2017**, *10*, 18. [CrossRef]
15. Litchfield, D.W. Protein kinase CK2: Structure, regulation and role in cellular decisions of life and death. *Biochem. J.* **2003**, *369*, 1–15. [CrossRef]
16. Guerra, B.; Issinger, O.G. Protein kinase CK2 and its role in cellular proliferation, development and pathology. *Electrophoresis* **1999**, *20*, 391–408.
17. Ahmad, K.A.; Wang, G.; Unger, G.; Slaton, J.; Ahmed, K. Protein kinase CK2- A key suppressor of apoptosis. *Adv. Enzyme Regul.* **2008**, *48*, 179–187. [PubMed]
18. Niefind, K.; Guerra, B.; Ermakowa, I.; Issinger, O.G. Crystal structure of human protein kinase CK2: Insights into basic properties of the CK2 holoenzyme. *EMBO J.* **2001**, *20*, 5320–5331. [CrossRef]
19. Ferrer-Font, L.; Alcaraz, E.; Plana, M.; Candiota, A.P.; Itarte, E.; Arús, C. Protein Kinase CK2 Content in GL261 Mouse Glioblastoma. *Pathol. Oncol. Res.* **2016**, *22*, 633–637. [CrossRef] [PubMed]
20. Schmitt, B.M.; Boewe, A.S.; Götz, C.; Philipp, S.E.; Urbschat, S.; Oertel, J.; Menger, M.D.; Laschke, M.W.; Ampofo, E. CK2 Activity Mediates the Aggressive Molecular Signature of Glioblastoma Multiforme by Inducing Nerve/Glial Antigen (NG)2 Expression. *Cancers* **2021**, *13*, 1678. [CrossRef]
21. Ji, H.; Lu, Z. The role of protein kinase CK2 in glioblastoma development. *Clin. Cancer Res.* **2013**, *19*, 6335–6337. [CrossRef]
22. Ladha, J.; Donakonda, S.; Agrawal, S.; Thota, B.; Srividya, M.R.; Sridevi, S.; Arivazhagan, A.; Thennarasu, K.; Balasubramaniam, A.; Chandramouli, B.A.; et al. Glioblastoma-specific protein interaction network identifies PP1A and CSK21 as connecting molecules between cell cycle-associated genes. *Cancer Res.* **2010**, *70*, 6437–6447. [CrossRef]
23. He, J.; Huang, Z.; Han, L.; Gong, Y.; Xie, C. Mechanisms and management of 3rd-generation EGFR-TKI resistance in advanced non-small cell lung cancer (Review). *Int. J. Oncol.* **2021**, *59*, 90. [CrossRef]
24. Ferrer-Font, L.; Villamanan, L.; Arias-Ramos, N.; Vilardell, J.; Plana, M.; Ruzzene, M.; Pinna, L.A.; Itarte, E.; Arus, C.; Candiota, A.P. Targeting Protein Kinase CK2: Evaluating CX-4945 Potential for GL261 Glioblastoma Therapy in Immunocompetent Mice. *Pharmaceuticals* **2017**, *10*, 24. [CrossRef]

25. Siddiqui-Jain, A.; Drygin, D.; Streiner, N.; Chua, P.; Pierre, F.; O'Brien, S.E.; Bliesath, J.; Omori, M.; Huser, N.; Ho, C.; et al. CX-4945, an Orally Bioavailable Selective Inhibitor of Protein Kinase CK2, Inhibits Prosurvival and Angiogenic Signaling and Exhibits Antitumor Efficacy. *Cancer Res.* **2010**, *70*, 10288–10298. [CrossRef]
26. Kim, H.; Lee, K.S.; Kim, A.K.; Choi, M.; Choi, K.; Kang, M.; Chi, S.W.; Lee, M.S.; Lee, J.S.; Lee, S.Y.; et al. A chemical with proven clinical safety rescues Down-syndrome-related phenotypes in through DYRK1A inhibition. *Dis. Model. Mech.* **2016**, *9*, 839–848.
27. Wells, C.I.; Drewry, D.H.; Pickett, J.E.; Tjaden, A.; Kramer, A.; Muller, S.; Gyenis, L.; Menyhart, D.; Litchfield, D.W.; Knapp, S.; et al. Development of a potent and selective chemical probe for the pleiotropic kinase CK2. *Cell Chem. Biol.* **2021**, *28*, 546–558. [CrossRef]
28. Pierre, F.; Chua, P.C.; O'Brien, S.E.; Siddiqui-Jain, A.; Bourbon, P.; Haddach, M.; Michaux, J.; Nagasawa, J.; Schwaebe, M.K.; Stefan, E.; et al. Pre-clinical characterization of CX-4945, a potent and selective small molecule inhibitor of CK2 for the treatment of cancer. *Mol. Cell. Biochem.* **2011**, *356*, 37–43. [CrossRef]
29. Kim, H.; Choi, K.; Kang, H.; Lee, S.Y.; Chi, S.W.; Lee, M.S.; Song, J.; Im, D.; Choi, Y.; Cho, S. Identification of a Novel Function of CX-4945 as a Splicing Regulator. *PLoS ONE* **2014**, *9*, e94978.
30. Hegde, M.M.; Palkar, P.; Mutalik, S.P.; Mutalik, S.; Goda, J.S.; Rao, B.S.S. Enhancing glioblastoma cytotoxicity through encapsulating O6-benzylguanine and temozolomide in PEGylated liposomal nanocarrier: An in vitro study. *3 Biotech* **2024**, *14*, 275. [CrossRef]
31. Schmitt, B.M.; Boewe, A.S.; Becker, V.; Nalbach, L.; Gu, Y.; Götz, C.; Menger, M.D.; Laschke, M.W.; Ampofo, E. Protein Kinase CK2 Regulates Nerve/Glial Antigen (NG)2-Mediated Angiogenic Activity of Human Pericytes. *Cells* **2020**, *9*, 1546.
32. Götz, C.; Gratz, A.; Kucklaender, U.; Jose, J. TF A novel cell-permeable and selective inhibitor of human protein kinase CK2 induces apoptosis in the prostate cancer cell line LNCaP. *Biochim. Biophys. Acta* **2012**, *1820*, 970–977. [CrossRef]
33. Schnitzler, A.; Gratz, A.; Bollacke, A.; Weyrich, M.; Kucklander, U.; Wunsch, B.; Götz, C.; Niefind, K.; Jose, J. A pi-Halogen Bond of Dibenzofuranones with the Gatekeeper Phe113 in Human Protein Kinase CK2 Leads to Potent Tight Binding Inhibitors. *Pharmaceuticals* **2018**, *11*, 23.
34. Rumler, H.; Schmithals, C.; Werner, C.; Bollacke, A.; Aichele, D.; Götz, C.; Niefind, K.; Wünsch, B.; Jose, J. Discovery of 7,9-Dibromo-dihydrodibenzofuran as a Potent Casein Kinase 2 (CK2) Inhibitor: Synthesis, Biological Evaluation, and Structural Studies on E-/Z-Isomers. *ACS Pharmacol. Transl. Sci.* **2024**, *7*, 3846–3866. [CrossRef]
35. Pucko, E.B.; Ostrowski, R.P. Inhibiting CK2 among Promising Therapeutic Strategies for Gliomas and Several Other Neoplasms. *Pharmaceutics* **2022**, *14*, 331. [CrossRef]
36. Zheng, Y.; McFarland, B.C.; Drygin, D.; Yu, H.; Bellis, S.L.; Kim, H.; Bredel, M.; Benveniste, E.N. Targeting protein kinase CK2 suppresses prosurvival signaling pathways and growth of glioblastoma. *Clin. Cancer Res.* **2013**, *19*, 6484–6494. [CrossRef]
37. Israel, I.; Blass, G.; Reiners, C.; Samnick, S. Validation of an amino-acid-based radionuclide therapy plus external beam radiotherapy in heterotopic glioblastoma models. *Nucl. Med. Biol.* **2011**, *38*, 451–460. [CrossRef]
38. Haddad, A.F.; Young, J.S.; Amara, D.; Berger, M.S.; Raleigh, D.R.; Aghi, M.K.; Butowski, N.A. Mouse models of glioblastoma for the evaluation of novel therapeutic strategies. *Neurooncol. Adv.* **2021**, *3*, vdab100. [CrossRef]
39. Barone, T.A.; Burkhart, C.A.; Safina, A.; Haderski, G.; Gurova, K.V.; Purmal, A.A.; Gudkov, A.V.; Plunkett, R.J. Anticancer drug candidate CBL0137, which inhibits histone chaperone FACT, is efficacious in preclinical orthotopic models of temozolomide-responsive and -resistant glioblastoma. *Neuro-Oncol.* **2017**, *19*, 186–196.
40. D'Amore, C.; Borgo, C.; Sarno, S.; Salvi, M. Role of CK2 inhibitor CX-4945 in anti-cancer combination therapy—Potential clinical relevance. *Cell. Oncol.* **2020**, *43*, 1003–1016.
41. Teuscher, K.B.; Zhang, M.; Ji, H. A Versatile Method to Determine the Cellular Bioavailability of Small-Molecule Inhibitors. *J. Med. Chem.* **2017**, *60*, 157–169. [CrossRef]
42. Loewe, S. The problem of synergism and antagonism of combined drugs. *Arzneimittelforschung* **1953**, *3*, 285–290.
43. Zheng, S.; Wang, W.; Aldahdooh, J.; Malyutina, A.; Shadbahr, T.; Tanoli, Z.; Pessia, A.; Tang, J. SynergyFinder Plus: Toward Better Interpretation and Annotation of Drug Combination Screening Datasets. *Genomics Proteomics Bioinformatics* **2022**, *20*, 587–596. [CrossRef]
44. Oronsky, B.; Reid, T.R.; Oronsky, A.; Sandhu, N.; Knox, S.J. A Review of Newly Diagnosed Glioblastoma. *Front. Oncol.* **2020**, *10*, 574012. [CrossRef]
45. Pyerin, W.; Ackermann, K. The genes encoding human protein kinase CK2 and their functional links. *Prog. Nucleic Acid Res. Mol. Biol.* **2003**, *74*, 239–273. [CrossRef]
46. Borgo, C.; Franchin, C.; Scalco, S.; Bosello-Travain, V.; Donella-Deana, A.; Arrigoni, G.; Salvi, M.; Pinna, L.A. Generation and quantitative proteomics analysis of CK2a/a'$^{(-/-)}$ cells. *Sci. Rep.* **2017**, *7*, 42409. [CrossRef]
47. Liu, X.; Chen, J.; Li, W.; Hang, C.; Dai, Y. Inhibition of Casein Kinase II by CX-4945, But Not Yes-associated protein (YAP) by Verteporfin, Enhances the Antitumor Efficacy of Temozolomide in Glioblastoma. *Transl. Oncol.* **2020**, *13*, 70–78. [CrossRef]

48. Wickström, M.; Dyberg, C.; Milosevic, J.; Einvik, C.; Calero, R.; Sveinbjörnsson, B.; Sandén, E.; Darabi, A.; Siesjö, P.; Kool, M.; et al. Wnt/β-catenin pathway regulates MGMT gene expression in cancer and inhibition of Wnt signalling prevents chemoresistance. *Nat. Commun.* **2015**, *6*, 8904. [CrossRef]
49. Liu, T.; Li, A.; Xu, Y.; Xin, Y. Momelotinib sensitizes glioblastoma cells to temozolomide by enhancement of autophagy via JAK2/STAT3 inhibition. *Oncol. Rep.* **2019**, *41*, 1883–1892. [CrossRef]
50. Shi, F.; Guo, H.; Zhang, R.; Liu, H.; Wu, L.; Wu, Q.; Liu, J.; Liu, T.; Zhang, Q. The PI3K inhibitor GDC-0941 enhances radiosensitization and reduces chemoresistance to temozolomide in GBM cell lines. *Neuroscience* **2017**, *346*, 298–308. [CrossRef]
51. Gerlach, S.L.; Metcalf, J.S.; Dunlop, R.A.; Banack, S.A.; Her, C.; Krishnan, V.V.; Göransson, U.; Gunasekera, S.; Slazak, B.; Cox, P.A. Kalata B1 Enhances Temozolomide Toxicity to Glioblastoma Cells. *Biomedicines* **2024**, *12*, 2216. [CrossRef]
52. Borgo, C.; D'Amore, C.; Sarno, S.; Salvi, M.; Ruzzene, M. Protein kinase CK2: A potential therapeutic target for diverse human diseases. *Signal Transduct. Target. Ther.* **2021**, *6*, 183. [CrossRef]
53. Villamañan, L.; Martínez-Escardó, L.; Arús, C.; Yuste, V.J.; Candiota, A.P. Successful Partnerships: Exploring the Potential of Immunogenic Signals Triggered by TMZ, CX-4945, and Combined Treatment in GL261 Glioblastoma Cells. *Int. J. Mol. Sci.* **2021**, *22*, 3453. [CrossRef]
54. Nitta, R.T.; Bolin, S.; Luo, E.; Solow-Codero, D.E.; Samghabadi, P.; Purzner, T.; Aujla, P.S.; Nwagbo, G.; Cho, Y.J.; Li, G. Casein kinase 2 inhibition sensitizes medulloblastoma to temozolomide. *Oncogene* **2019**, *38*, 6867–6879. [CrossRef]
55. Cozza, G.; Pinna, L.A. Casein kinases as potential therapeutic targets. *Expert Opin. Ther. Targets* **2016**, *20*, 319–340. [CrossRef]
56. Battistutta, R.; Cozza, G.; Pierre, F.; Papinutto, E.; Lolli, G.; Sarno, S.; O'Brien, S.E.; Siddiqui-Jain, A.; Haddach, M.; Anderes, K.; et al. Unprecedented selectivity and structural determinants of a new class of protein kinase CK2 inhibitors in clinical trials for the treatment of cancer. *Biochemistry* **2011**, *50*, 8478–8488. [CrossRef]
57. Girardi, C.; Ottaviani, D.; Pinna, L.A.; Ruzzene, M. Different Persistence of the Cellular Effects Promoted by Protein Kinase CK2 Inhibitors CX-4945 and TDB. *Biomed Res. Int.* **2015**, *2015*, 185736. [CrossRef]
58. Cozza, G.; Girardi, C.; Ranchio, A.; Lolli, G.; Sarno, S.; Orzeszko, A.; Kazimierczuk, Z.; Battistutta, R.; Ruzzene, M.; Pinna, L.A. Cell-permeable dual inhibitors of protein kinases CK2 and PIM-1: Structural features and pharmacological potential. *Cell. Mol. Life Sci.* **2014**, *71*, 3173–3185. [CrossRef]
59. Ahmed, K.; Gerber, D.A.; Cochet, C. Joining the cell survival squad: An emerging role for protein kinase CK2. *Trends Cell Biol.* **2002**, *12*, 226–230. [CrossRef]
60. Bova, V.; Mannino, D.; Salako, A.E.; Esposito, E.; Filippone, A.; Scuderi, S.A. Casein Kinase 2 Inhibitor, CX-4945, Induces Apoptosis and Restores Blood-Brain Barrier Homeostasis in In Vitro and In Vivo Models of Glioblastoma. *Cancers* **2024**, *16*, 3936. [CrossRef]
61. Bliesath, J.; Huser, N.; Omori, M.; Bunag, D.; Proffitt, C.; Streiner, N.; Ho, C.; Siddiqui-Jain, A.; O'Brien, S.E.; Lim, J.K.; et al. Combined Inhibition of EGFR and CK2 Augments the Attenuation of PI3K-Akt-mTOR Signaling and the Killing of Cancer Cells. *Cancer Lett.* **2012**, *322*, 113–124. [CrossRef]
62. Price, M.A.; Colvin Wanshura, L.E.; Yang, J.; Carlson, J.; Xiang, B.; Li, G.; Ferrone, S.; Dudek, A.Z.; Turley, E.A.; McCarthy, J.B. CSPG4, a potential therapeutic target, facilitates malignant progression of melanoma. *Pigment Cell Melanoma Res.* **2011**, *24*, 1148–1157. [CrossRef]
63. Atkinson, E.L.; Iegre, J.; Brear, P.D.; Zhabina, E.A.; Hyvönen, M.; Spring, D.R. Downfalls of Chemical Probes Acting at the Kinase ATP-Site: CK2 as a Case Study. *Molecules* **2021**, *26*, 1977. [CrossRef]
64. Gyenis, L.; Menyhart, D.; Cruise, E.S.; Jurcic, K.; Roffey, S.E.; Chai, D.B.; Trifoi, F.; Fess, S.R.; Desormeaux, P.J.; Núñez de Villavicencio Díaz, T.; et al. Chemical Genetic Validation of CSNK2 Substrates Using an Inhibitor-Resistant Mutant in Combination with Triple SILAC Quantitative Phosphoproteomics. *Front. Mol. Biosci.* **2022**, *9*, 909711. [CrossRef]
65. Liu, L.; Yang, S.; Lin, K.; Yu, X.; Meng, J.; Ma, C.; Wu, Z.; Hao, Y.; Chen, N.; Ge, Q.; et al. Sp1 induced gene TIMP1 is related to immune cell infiltration in glioblastoma. *Sci. Rep.* **2022**, *12*, 11181. [CrossRef]
66. Yu, Y.; Cao, F.; Xiong, Y.; Zhou, H. SP1 transcriptionally activates NLRP6 inflammasome and induces immune evasion and radioresistance in glioma cells. *Int. Immunopharmacol.* **2021**, *98*, 107858. [CrossRef]
67. Zhang, S.; Kim, K.H. Protein kinase CK2 down-regulates glucose-activated expression of the acetyl-CoA carboxylase gene. *Arch. Biochem. Biophys.* **1997**, *338*, 227–232. [CrossRef]
68. Krehan, A.; Ansuini, H.; Bőcher, O.; Grein, S.; Wirkner, U.; Pyerin, W. Transcription factors Ets1, NF-kappaB, and Sp1 are major determinants of the promoter activity of the human protein kinase CK2α gene. *J. Biol. Chem.* **2000**, *275*, 18327–18336. [CrossRef]
69. Sahoo, G.; Samal, D.; Khandayataray, P.; Murthy, M.K. A Review on Caspases: Key Regulators of Biological Activities and Apoptosis. *Mol. Neurobiol.* **2023**, *60*, 5805–5837. [CrossRef]
70. Turowec, J.P.; Duncan, J.S.; Gloor, G.B.; Litchfield, D.W. Regulation of caspase pathways by protein kinase CK2: Identification of proteins with overlapping CK2 and caspase consensus motifs. *Mol. Cell. Biochem.* **2011**, *356*, 159–167. [CrossRef]

71. Turowec, J.P.; Vilk, G.; Gabriel, M.; Litchfield, D.W. Characterizing the convergence of protein kinase CK2 and caspase-3 reveals isoform-specific phosphorylation of caspase-3 by CK2alpha': Implications for pathological roles of CK2 in promoting cancer cell survival. *Oncotarget* **2013**, *4*, 560–571. [CrossRef]
72. Kaufmann, S.H.; Desnoyers, S.; Ottaviano, Y.; Davidson, N.E.; Poirier, G.G. Specific proteolytic cleavage of poly(ADP-ribose) polymerase: An early marker of chemotherapy-induced apoptosis. *Cancer Res.* **1993**, *53*, 3976–3985. [PubMed]
73. Soldani, C.; Lazzè, M.C.; Bottone, M.G.; Tognon, G.; Biggiogera, M.; Pellicciari, C.E.; Scovassi, A.I. Poly(ADP-ribose) polymerase cleavage during apoptosis: When and where? *Exp. Cell Res.* **2001**, *269*, 193–201. [CrossRef] [PubMed]
74. Birus, R.; El-Awaad, E.; Ballentin, L.; Alchab, F.; Aichele, D.; Ettouati, L.; Götz, C.; Le Borgne, M.; Jose, J. 4,5,7-Trisubstituted indeno [1,2-b]indole inhibits CK2 activity in tumor cells equivalent to CX-4945 and shows strong anti-migratory effects. *FEBS Open Bio* **2022**, *12*, 394–411.
75. Rahnel, H.; Viht, K.; Lavogina, D.; Mazina, O.; Haljasorg, T.; Enkvist, E.; Uri, A. A Selective Biligand Inhibitor of CK2 Increases Caspase-3 Activity in Cancer Cells and Inhibits Platelet Aggregation. *ChemMedChem* **2017**, *12*, 1723–1736. [CrossRef] [PubMed]
76. Schwind, L.; Schetting, S.; Montenarh, M. Inhibition of protein kinase CK2 prevents adipogenic differentiation of mesenchymal stem cells like C3H/10T1/2 cells. *Pharmaceuticals* **2017**, *10*, 22.
77. Faust, M.; Schuster, N.; Montenarh, M. Specific binding of protein kinase CK2 catalytic subunits to tubulin. *FEBS Lett.* **1999**, *462*, 51–56. [CrossRef]
78. Münstermann, U.; Fritz, G.; Seitz, G.; Lu, Y.P.; Schneider, H.R.; Issinger, O.G. Casein kinase II is elevated in solid human tumours and rapidly proliferating non-neoplastic tissue. *Eur. J. Biochem.* **1990**, *189*, 251–257. [CrossRef]
79. Pack, M.; Götz, C.; Wrublewsky, S.; Montenarh, M. SGC-CK2-1 Is an Efficient Inducer of Insulin Production and Secretion in Pancreatic beta-Cells. *Pharmaceutics* **2022**, *14*, 19.